

# Recent Results from Super-Kamiokande

H. Sekiya (for the Super-Kamiokande Collaboration)

Kamioka Observatory, Institute for Cosmic Ray Research, University of Tokyo  
456 Higashi-Mozumi, Kamioka, Gifu, 506-1205 JAPAN

The recent results on the oscillation analyses of solar neutrino and the atmospheric neutrino measurements in Super-Kamiokande are presented. Recent status of the detector is also reported.

## 1. INTRODUCTION

Super-Kamiokande (SK) is a water Cherenkov detector containing 50,000 tons of pure water. It is located 1000 meters underground (2,700 meters of water equivalent) in Kamioka zinc mine in Japan. The detector consists of a main inner detector and an outer veto detector. Both detectors are contained within a cylindrical stainless steel tank 39.3 m in diameter 41.4 m in height. The usual fiducial mass for neutrino measurements is 22.5 ktons with boundaries 2.0 m from the inner surface.

The first phase of the SK (SK-I) started in April, 1996, and terminated in July, 2001. A total of 11,146 PMTs with 20-inch diameter photocathodes provided active light collection over 40% of the surface of the inner detector. Then, in spite of the loss of numerous PMTs in an accident, the second phase (SK-II) started in December, 2002. A total of 5,182 20-inch PMTs, each protected by acrylic and fiber-reinforced plastic (FRP) cases, were mounted on the inner detector, providing 19% photocathode coverage during this period. SK-II ran until October 2005. In the analysis of the SK-II data, analysis methods had to be revised due to the loss of detector sensitivity, however it turned out that the revised method also effective in the SK-I data analysis.

In July 2006, SK detector was totally recovered with 40% photocathode coverage and started taking data as SK-III. During this phase, the water flow in the tank had been tuned up and the low energy background was reduced. In order to further enhance its performance, SK-III was terminated in August 2008, and the readout electronics and online data acquisition system were upgraded. The fourth phase (SK-IV) started in September 2008.

In this paper we report updated SK-I + SK-II results of solar and atmospheric neutrino oscillation analyses and the detector status of SK-III and SK-IV.

## 2. SOLAR NEUTRINO (SK-I and SK-II)

The advantages of SK in the solar neutrino observation are the time variation measurement, the direction-sensitivity, and the very precise measurement of its spectrum due to the well calibrated energy of recoil electrons [1].

The solar neutrino flux can be derived from the extracted number of signal events by fitting signal+background shapes to the recoil angle distribution relative to the Sun ( $\cos \theta_{\text{sun}}$ ). The observed solar neutrino flux in each phase of SK is summarized in Table

reftab: ux. The SK-II flux value is statistically consistent with the SK-I value. Figure 1 shows the SK-II observed energy spectrum divided by the expected spectrum without oscillation determined from the BP2004 SSM [2]. The line through the spectrum represents the total SK-I average. SK-II shows excellent agreement with SK-I.

Phase	Live time (days)	Energy Range (MeV)	Number of signals	Flux ( $10^6 \text{ cm}^{-2} \text{ sec}^{-1}$ )
SK-II	791	7.0-20.0	$7212.8^{+152.9}_{-150.9}$ (stat) $^{+483.3}_{-461.6}$ (sys)	$2.38 \pm 0.05$ (stat) $^{+0.16}_{-0.15}$ (sys)
SK-I	1496	5.0-20.0	$22404 \pm 226$ (stat) $^{+784}_{-717}$ (sys)	$2.35 \pm 0.02$ (stat) $0.08$ (sys)

Table I: Observed solar neutrino flux in SK-I and SK-II

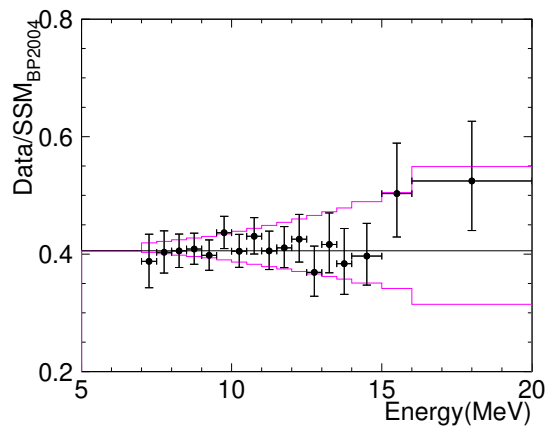


Figure 1: Ratio of observed and expected energy spectra. The purple lines represent a 1 sigma level of the energy correlated systematic errors. The black line represents the SK-I 1496-day average and shows agreement with SK-II.

The determination of the solar neutrino oscillation parameters in SK-I and SK-II is accomplished in the same way [3]. Two neutrino oscillation is assumed and for each set of oscillation parameters, a  $\chi^2$  minimization of the total  $^8\text{B}$  and hep neutrino flux is fit to the data. This yields exclude regions, while by constraining the  $^8\text{B}$  flux to the total NC flux value from SNO [4], allowed regions can be obtained. Figure 2 shows both excluded and allowed regions at 95% confidence level.

The combination of other solar neutrino experiments such as SNO and radiochemical results (Homestake, GALLEX and SAGE) with the SK combined analysis is also accomplished and shown Figure 2. The best fit parameter set is  $\tan^2 \theta = 0.40$  and  $m^2 = 6.03 \times 10^{-5} \text{eV}^2$ .

### 3. ATMOSPHERIC NEUTRINO (SK-I and SK-II)

Super-Kamiokande has reported that the atmospheric neutrino data are well consistent with the pure  $\delta$  two flavor oscillation scheme [6]. Recently  $\delta$  oscillation analyses for zenith angle distributions and L/E distribution are re-performed using SK-I and SK-II data with improved analysis methods to get more stringent constraint on the oscillation parameters. The changes to the simulation include: an update of the atmospheric neutrino flux model to the "Honda06" model [7]; various modifications to the neutrino interaction model, NEUT [8] (e.g., change of quasi-elastic and single pion axial mass to  $M_A = 1.2 \text{ GeV}$ , addition of lepton mass effects for charged-current single pion production, and addition of the pion-less delta decay channel  $\pi \rightarrow N \gamma$ ); improvements to the detector simulation model of light reflections and scattering; better tuning of outer detector parameters in the simulation; and improvements in the ring counting algorithm. Additionally, at the time of re-analysis, the systematic uncertainties were re-evaluated and a few new uncertainties were added.

Atmospheric neutrino data are categorized into fully-contained (FC), partially-contained (PC), and upward-going muon (UP) events. In the zenith angle analysis, 1489 days of SK-I FC/PC data 1646 days of UP SK-I data, 799 days of SK-II FC/PC data and 828 days of UP SK-II data are used. All samples are divided in 10 zenith angle bins. The definition of the event bins are same as SK-I and SK-II, and 400 bins for SK-I and 350 bins for SK-II are used in the analysis. The number of observed events in each of 750 bins is compared with the Monte Carlo expectation. A  $\chi^2$  value is defined according to the Poisson probability distribution. In the fitting, the expected number of events in each bin is recalculated to account for 90 systematic errors, which come from the uncertainty of the neutrino flux model, neutrino cross-section model, event selection, and the detector response. Figure 3 shows contours of allowed parameter regions. Best fit parameter set is  $\sin^2 2\theta = 1.02$  and  $m^2 = 2.1 \times 10^{-3} \text{eV}^2$ .

In the L/E analysis, more strict selection criteria are applied to the subsample data, because a good resolution for

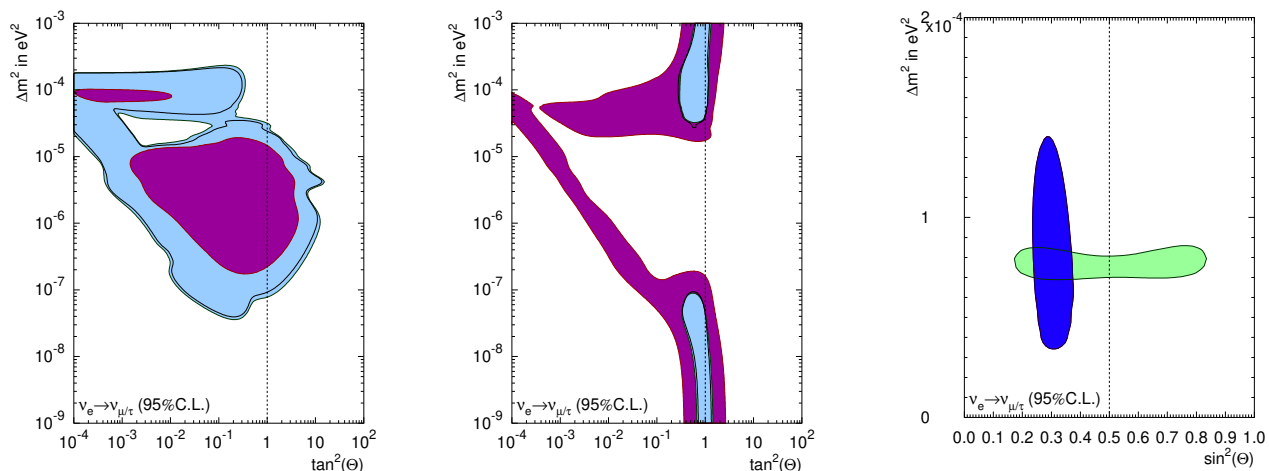


Figure 2: The left plot shows SK excluded areas. The purple region is SK-II and the light blue region is SK-I with SK-II. The black line shows SK-I only, and evidence of increased exclusion can be seen with the addition of SK-II data. The center plot shows SK allowed regions (same representative colors as the exclusion contours) with the  $^8\text{B}$  flux constrained to the SNO total flux measurement. The hep flux is a free parameter. The right plot shows the SK-I and SK-II combined contour with SNO and radiochemical solar experimental data (blue contour). The green contour is the KamLAND [5] electron anti-neutrino oscillation result.

neutrino flight pathlength,  $L$ , and energy,  $E$ , is required when trying to observe the expected dip in the  $L/E$  spectrum due to oscillations. 1468 days of SK-I FC/PC-like events and 799 days of SK-II FC/PC-like events are used and divided in 43 bins of  $\log_{10}(L/E)$  (km/GeV). The results of a minimum  $\chi^2$  fit to the 43 bins with 29 systematic error terms are shown in Figure 3. Best fit parameter set is  $\sin^2 2\theta = 1.04$  and  $m^2 = 2.2 \times 10^{-3} \text{eV}^2$ .

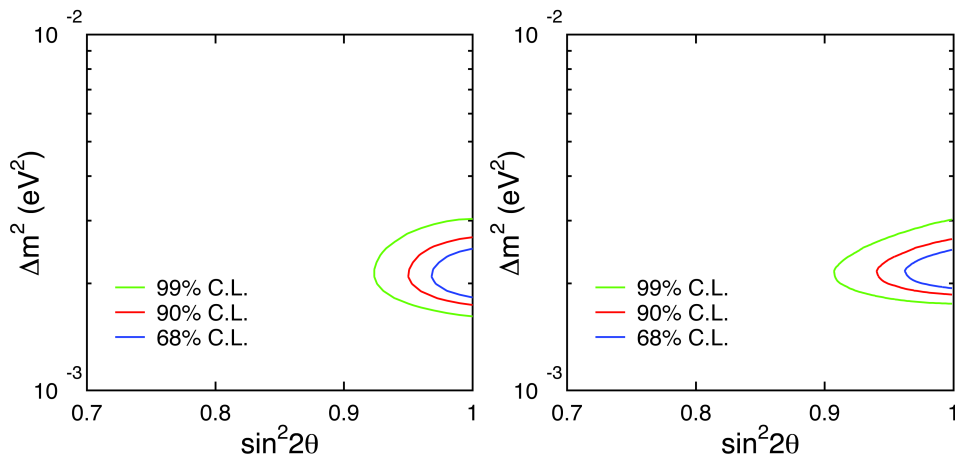


Figure 3: The left plot shows allowed oscillation parameters by the zenith angle analysis and the right plot shows the ones by the  $L/E$  analysis.

## 4. STATUS OF THE DETECTOR (SK-III and SK-IV)

The lower energy threshold of SK-I had been limited to around 5.0 MeV due to residual radon in the water emanated from the PMT/FRP, therefore the water purification system was upgraded and the water flow in SK tank had been tuned in the SK-III phase. Figure 4 shows  $\cos\theta_{\text{sun}}$  distribution of the central region. In the 5.0-5.5 MeV region, background event rate of SK-III is about 1/3 of that of SK-I, while the signal rate looks similar. Based on this background reduction, the trigger threshold had been lowered since April 2008, and 100% trigger efficiency at 4.5 MeV was achieved in the last period of SK-III.

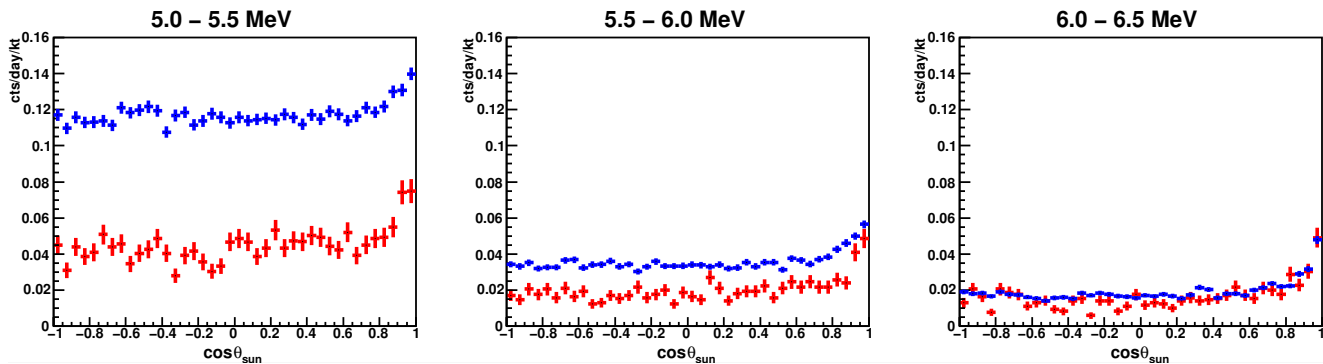


Figure 4: The electron recoil angle distribution relative to the Sun in the central region of SK tank ( $16 > z > -7.5\text{m}$ ,  $r < 11\text{m}$ ). The blue line shows SK-I and the red line shows SK-III.

In order to further enhance its performance, new electronics system using custom ASIC had been developed and was installed to SK. In the new system, all PMT hits are sent to the front-end DAQ computers by a periodic timing signal and software triggers are applied to select interesting event windows. SK has started taking data of every hit without any hardware trigger as "SK-IV" since September 2008. This enables higher speed data taking, much lower energy threshold and wider dynamic range with aiming at increasing detection efficiency of supernova burst neutrino, detecting the spectrum distortion of low energy  $^8\text{B}$  solar neutrino, and improving the energy resolution of multi-GeV atmospheric neutrino.

## 5. CONCLUSION

Super-Kamiokande (SK-I,II,III) have been operated successfully, and more than 10 years of dataset for solar and atmospheric neutrino are accumulated. With the combined SK-I and SK-II dataset, the best  $\theta$  oscillation parameter set is found at  $\tan^2 = 0.40$  and  $m^2 = 6.03 \times 10^5 \text{eV}^2$  in the solar global analysis and at  $\sin^2 2 = 1.02$  and  $m^2 = 2.1 \times 10^3 \text{eV}^2$  in the atmospheric zenith angle analysis. In SK-III, the background rate in the low energy region was reduced and SK-IV has just started since September 2008 with upgraded electronics. Super-Kamiokande will continue to observe every predicted effect and measure mixing angles. In addition, high-statistics data sets make it feasible to search for sub-dominant, exotic, and non-oscillation physics.

## References

- [1] M. Nakahata et al., Nucl. Instr. Meth. A 421 (1999) 113.
- [2] J.N. Bahcall and M.H. Pionneault, Phys. Rev. Lett. 92 (2004) 121301.
- [3] J.P. C. ravens et al., Phys. Rev. D 78 (2008) 032002.
- [4] S.N. Ahmed et al., Phys. Rev. Lett. 92 (2004) 181301.
- [5] T. Araki et al., Phys. Rev. Lett. 94 (2005) 081801.
- [6] Y. Ashie et al., Phys. Rev. D 71 (2005) 112005.
- [7] M. Honda et al., Phys. Rev. D 75 (2007) 043006.
- [8] Y. Hayato, Nucl. Phys. B (Proc. Suppl.) 112 (2002) 171.